The Plant Cell, Vol. 11, 1319–1336, July 1999, www.plantcell.org © 1999 American Society of Plant Physiologists

Epigenetic Interactions among Three *dTph1* Transposons in Two Homologous Chromosomes Activate a New Excision–Repair Mechanism in Petunia

Adèle van Houwelingen,[1] Erik Souer, Jos Mol, and Ronald Koes[2]

Department of Genetics, Institute for Molecular Biological Sciences, Vrije Universiteit, BioCentrum Amsterdam, de Boelelaan 1087, 1081 HV, Amsterdam, The Netherlands

Unstable *anthocyanin3* (*an3*) alleles of petunia with insertions of the *Activator*/*Dissociation*–like transposon *dTph1* fall into two classes that differ in their genetic behavior. Excision of the (single) *dTph1* insertion from class 1 *an3* alleles results in the formation of a footprint, similar to the "classical" mechanism observed for excisions of maize and snapdragon transposons. By contrast, *dTph1* excision and gap repair in class 2 *an3* alleles occurs via a newly discovered mechanism that does not generate a footprint at the empty donor site. This novel mechanism depends on the presence of two additional *dTph1* elements: one located in *cis*, 30 bp upstream of the *an3* translation start in the same *an3* allele, and a homologous copy, which is located in *trans* in the homologous *an3* allele. Absence of the latter *dTph1* element causes a heritable suppression of *dTph1* excision–repair from the homologous *an3* allele by the novel mechanism, which to some extent resembles paramutation. Thus, an epigenetic interaction among three *dTph1* copies activates a novel recombination mechanism that eliminates a transposon insertion.

INTRODUCTION

The best characterized class of transposons comprises elements with short terminal inverted repeats that transpose via a "cut-and-paste" mechanism. This class includes, for example, Tn*7* and Tn*10* of *Escherichia coli*, *Activator* (*Ac*), *Dissociation* (*Ds*), and *Enhancer*/*Suppressor-Mutator* (*En*/*Spm*) elements from maize, various *Tam* elements from snapdragon, *P* and *Hobo* elements from Drosophila, and various families of *Tc* elements from *Caenorhabditis elegans*. In addition, an increasing amount of evidence indicates that the intervening sequences, which are excised from genes encoding immunoglobulins and T-cell receptors to join variable (V), diversity (D), and joining (J) segments, originate from a cut-and-paste transposon (Agrawel et al., 1998; Hiom et al., 1998; reviewed in Roth and Craig, 1998).

The mobility of these transposable elements is controlled by a variety of mechanisms, all of which regulate expression of the recombinase enzyme(s) involved. For instance, in mammals, V(D)J joining is restricted to certain lymphoid cells, because other cell types do not express the proteins RAG1 and RAG2 that initiate the joining reaction (Oetinger et al., 1990). In Drosophila, differential splicing of the P transposase mRNA yields either a functional transposase (in the germ line) or a truncated version of the transposase (in the soma) that represses transposase gene transcription and transposition. Certain deletion derivatives of *P* repress transposition, presumably by a similar mechanism (reviewed in Engels, 1996). Also, epigenetic mechanisms contribute to the regulation of transposition frequency. The variegated flower color specified by the *Tam2* insertion allele *nivea-44* of snapdragon is inherited in a non-Mendelian manner, suggesting that one or more epigenetic factors regulate *Tam2* activity (Hudson et al., 1987; Krebbers et al., 1987). In maize, the heritable inactivation of *Ac* and *Spm* elements is associated with increased methylation and reduced transposase expression (Banks et al., 1988; Brutnell and Dellaporta, 1994). At low frequency, the introduction of an active transposon copy can result in demethylation and reactivation of the repressed element (Banks et al., 1988; Fedoroff, 1989; Schwartz, 1989; Brutnell and Dellaporta, 1994; Brutnell et al., 1997). In the case of *Spm*, this interaction is mediated by the TNPA protein, which is expressed from the active *Spm* and binds, activates, and demethylates the promoter of the inactive *Spm* element (Schläppi et al., 1994).

Recent evidence shows that transposition and V(D)J joining, as well as replication of certain bacteriophages and retroviral integration, rely on the same basic chemistry for the breaking and joining of DNA segments. Hydrolytic nicking of DNA strands (in which H_2O acts as the nucleophile) generates free 3′ hydroxyl groups, which by nucleophilic attack

[1] Current address: Centre for Plant Reproduction Research (CPRO-DLO), Wageningen, The Netherlands.
[2] To whom correspondence should be addressed. E-mail koes@bio.vu.nl; fax 31-20-4447155.

engage in transesterification reactions and joining to the target DNA (reviewed in Craig, 1995; Roth and Craig, 1998). The differences in the products that are produced by distinct DNA transfer reactions depend on the site(s) and the strand(s) at which donor and target DNAs are cleaved. Presumably, because their free 3′ OH ends attack the top and bottom strand of the target DNA at a slightly different position, each transposon duplicates a characteristic number of nucleotides of the target site during integration. For instance, integration of *P* or *Ac* and related elements produces 8-bp target site duplications, whereas those produced by *En*/*Spm* and related transposons are 3 bp in length.

By analyzing (phenotypic) reversions of unstable transposon insertion alleles, one can monitor the excisions of these transposons. Strikingly, *P*, *Ac*, and *Tam* insertion alleles appear to revert by different mechanisms in their cognate hosts (reviewed in Rommens et al., 1993). This may be due to differences in the excision mechanism or in the mechanism that repairs the double strand excision-induced break.

The excision of a plant transposon usually results in the complete removal of transposon sequences and the formation of a so-called footprint (reviewed in Kunze et al., 1997). Generally, such footprints consist of remainders of the target site duplication. These are often separated by inverted copies of the target site. Typically, footprints created by *Ac*-like transposons lack at least one nucleotide in the axis of symmetry, whereas those created by transposons of the CACTA family (e.g., *Spm*) generally produce perfect palindromes. To explain these features, Coen et al. (1986) proposed that *Ac*-like and CACTA transposons excise by a 1-bp staggered and a blunt-ended cut, respectively, and that the DNA ends at the excision break form hairpin structures. After subsequent resolution of the hairpin by a second nick, the ends are ligated and a footprint is created. By using in vitro systems, it was shown that hairpin molecules indeed arise during V(D)J joining (van Gent et al., 1995, 1996) and Tn*10* excision (Kennedy et al., 1998) as a direct consequence of the mechanism by which the double-strand breaks (DSBs) are made.

Engels et al. (1990) showed that the (germinal) reversion frequency of unstable Drosophila alleles with *P* insertions depends on the structure of the allele on the homologous chromosome and proposed that excision gaps are repaired by a gene conversion–like mechanism, called DSB repair, that uses the homologous chromosome or sister chromatid as a template. The demonstration that marked sequences could be transferred from the homologous allele or a transgene into the empty donor site provided direct support for the DSB repair model (Gloor et al., 1991; Johnson-Schlitz and Engels, 1993). DSB repair also has been implicated in the repair of the gaps created by *Tc1* and *Tc3* elements in *C. elegans* germ line cells (Plasterk, 1991), even though these transposons are unrelated to *P*. Although the role of DSB repair in transposon excision in plants has not been directly investigated, some transposition events have been explained by invoking DSB repair. For instance, *Mutator* (*Mu*) elements of maize are thought to transpose by a (quasi)replicative mechanism in germinal cells, and the structure of *Mu* excision products fits with a DSB repair model (Lisch et al., 1995; Hsia and Schnable, 1996; Mathern and Hake, 1997). Even though reversion of *Ac* insertion alleles in maize does not display homolog dependency (Baran et al., 1992), it has been suggested that some excision products result from DSB repair (Chen et al., 1992; Rommens et al., 1993).

We recently generated by random transposon mutagenesis a series of mutant alleles for the *anthocyanin3* (*an3*) locus of petunia (van Houwelingen et al., 1998). This locus contains the gene coding for the enzyme flavanone 3β-hydroxylase (F3H), which is required for the synthesis of anthocyanin pigments in the flower. Consequently, stable *an3* mutants have nearly white flowers, whereas unstable *an3* mutants have nearly white flowers with colored revertant sectors and spots. Molecular analysis showed that the unstable *an3* alleles contained one or two insertions of either of the petunia transposons *dTph1* or *dTph2*. Both of these transposons are members of the *Ac* superfamily, because they duplicate 8 bp of target sequence when integrated and because the sequences of their terminal inverted repeats are similar to those of *Ac* and related transposons (Gerats et al., 1990; Kroon et al., 1994; van Houwelingen et al., 1998). Furthermore, the footprints left behind after *dTph1* and *dTph2* excision are similar to those found for other members of the *Ac* superfamily (Souer et al., 1996, 1998; de Vetten et al., 1997; Alfenito et al., 1998; this study). Both *dTph1* and *dTph2* are nonautonomous transposons because they are too small (284 and 177 bp, respectively) to encode their own transposase. Genetic mapping showed that transposition of *dTph1* requires the immobile *Act1* locus that may encode either the transposase or a host factor involved in transposition (Huits et al., 1994).

In this study, we show that *an3* alleles with a single transposon insertion (*dTph1* or *dTph2*) behave like unstable transposon insertion alleles in maize and snapdragon. Surprisingly, we found that the four unstable *an3* alleles harboring two *dTph1* elements revert preferentially via a novel mechanism. This mechanism relies on (epigenetic) interactions among three *dTph1* copies on the two homologous chromosomes and results in elimination of a *dTph1* insertion without leaving a footprint.

RESULTS

Analysis of Excision Alleles

Figures 1A and 1B summarize the flower phenotypes and the structures of mutant *an3* alleles. The transposon insertion alleles are all genetically unstable and undergo somatic and germinal transitions to new stable derivatives with activities ranging from wild type to null. Polymerase chain reac-

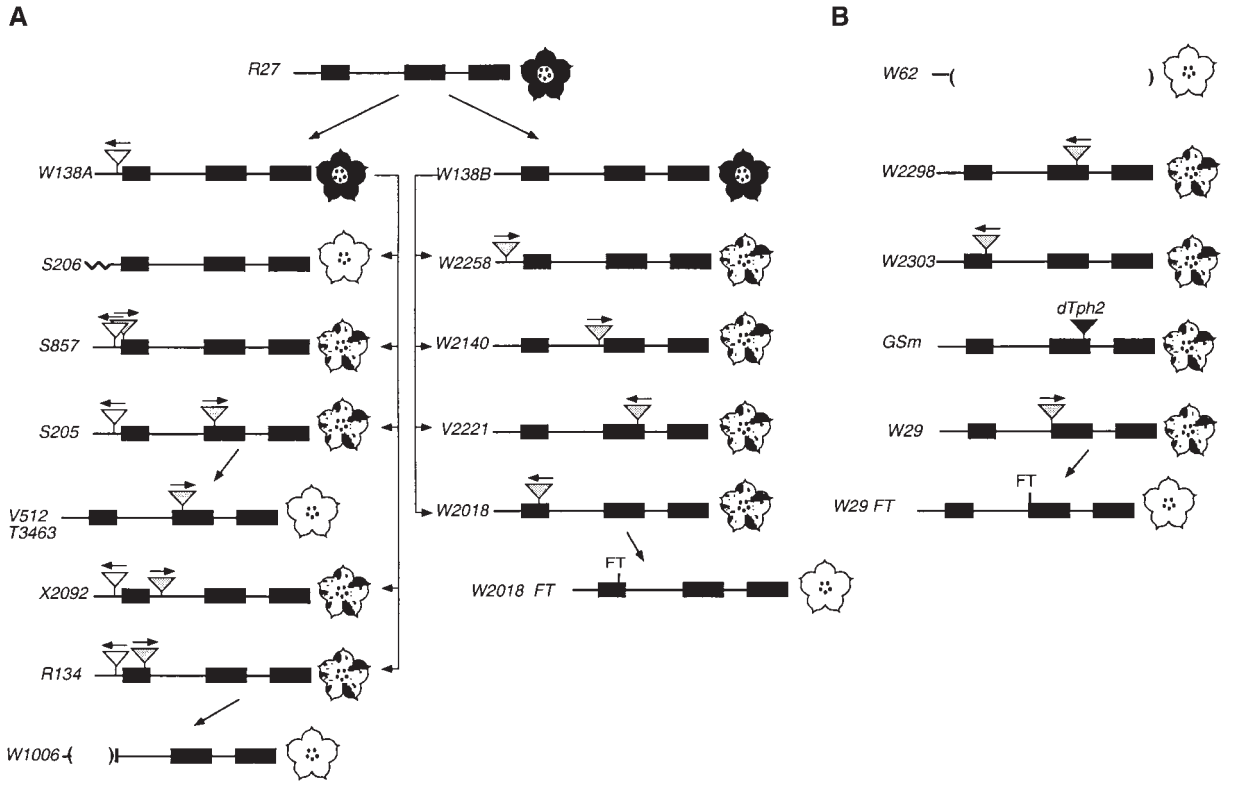

Figure 1. Schematic Showing the Structure and Genetic Relation of *an3* Alleles.

(A) The structure and pedigree of *an3* alleles isolated in the W138 genetic background.

(B) The structure of *an3* alleles isolated in various other genetic backgrounds.

Black boxes represent exon sequences. Positions of transposons are indicated by triangles; the arrows indicate their direction. The flowers show the phenotype for each allele when homozygous. Black, $An3^{+}$ (colored flowers); spotted, $an3^{mut}$ (flowers with red/pink spots on white background); white, $an3^{-}$ (nearly white flowers). The presence of a footprint is indicated with FT; the wavy line in *S206* represents DNA sequences that were fused to the *an3* locus by a large chromosomal rearrangement (a translocation or inversion). Deletions in the *an3* locus are indicated by empty regions flanked by parentheses. Note that *W138A* harbors a *dTph1* insertion (open triangle) 30 bp upstream of the translation start, which does not affect pigmentation of the flower on its own. The unstable alleles *R134*, *S205*, *S857*, and *X2092* are derived from *W138A* and harbor a second *dTph1* insertion (shaded triangle), downstream of the ATG, that is responsible for the mutant phenotype. *an3* alleles derived from *an3-W138B* have a single *dTph1* insertion. Details on the structural analysis of the transposon insertion alleles and the stable recessive alleles *W62*, *S206*, and *W1006* are documented elsewhere (van Houwelingen et al., 1998). The alleles *W29FT*, *V512*, *T3463*, and *W2018FT* were isolated during this work.

tion (PCR) analyses showed that these transitions correlated, with a few exceptions (see below), with excision of the transposon. To study the excision mechanism, we isolated and sequenced a series of such excision products.

For one set of *an3* alleles (termed class 1), we found that the wild-type sequence was rarely restored after excision of *dTph1* or *dTph2* and that a so-called transposon footprint was usually generated (Figure 2A). A partial reversion allele (called *W29FT*) in which *dTph1* had excised from *an3-W29* was identified by phenotype in progeny from self-pollinated *W29*/*W29* plants. Sequence analysis showed that *W29FT* contained a footprint that consisted of remainders of the duplicated 8-bp target site separated by inverted repetitions of part of the target site (Figure 2A). However, phenotypic selection of excision alleles may favor the recovery of certain excision alleles (those that partially or fully restore gene activity) over others. To avoid such a bias, we analyzed PCR-amplified somatic excision products from plants homozygous for the *dTph1* insertion alleles *W29*, *W2018*, *W2303*, *W2140*, *W2298*, *V2221*, and *W138A*. In all somatic excision products, transposon footprints were found that in structure resembled that in W29FT (Figure 2A).

Excisions of *dTph2* from the *an3-GSm* allele created footprints that were very similar to the *dTph1*-induced footprints (Figure 2A). In one case, we recovered a perfectly restored wild-type sequence. However, we believe that this is a rare

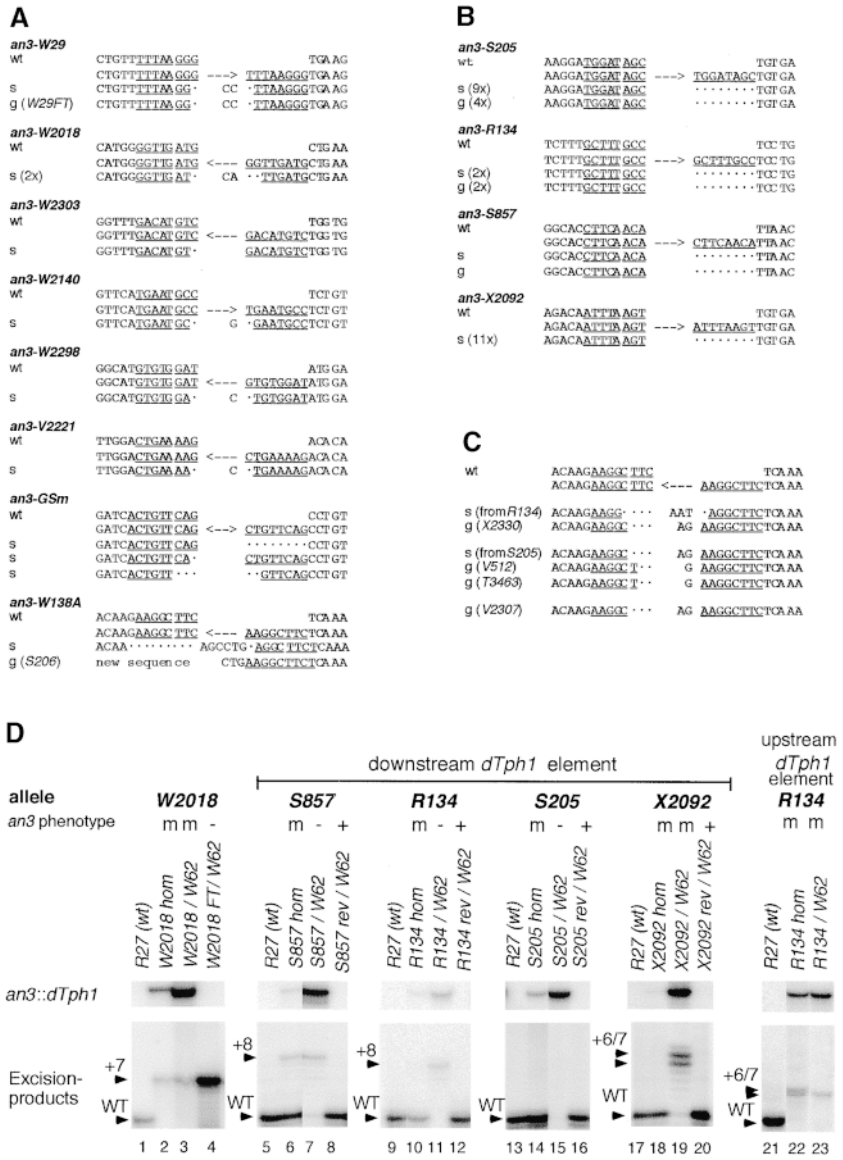

Figure 2. Excision Products Produced by Class 1 and Class 2 *an3* Alleles.

(A) Sequence analysis of PCR-amplified excision products generated by the transposon in class 1 *an3* alleles. For each *an3* allele, the position of the insertion is indicated by an arrow, and the direction is as given in Figure 1. The target site duplications flanking the transposon are underlined. Excision alleles are indicated with s (somatic excision) or g (germinal excision). Numbers in parentheses indicate the number of times that excision alleles with the given sequence were found. Black dots indicate missing base pairs of the target site duplication after excision of the element. For comparison, the wild-type sequences (wt) surrounding the insertion sites are also shown.

(B) Sequence analysis of PCR-amplified excision products generated by excision of the downstream *dTph1* element in class 2 *an3* alleles.

(C) Sequence analysis of PCR-amplified excision products generated by excision of the upstream *dTph1* element in a class 2 *an3* allele. The germinal excision allele *X2330* derived from *R134*, *V512* and *T3463* derived from *S205*, and *V2307* derived from *S857*.

(D) Analysis of PCR-amplified excision products of class 1 and class 2 alleles on 6% polyacrylamide gels. Excision products of the class 1 allele *W2018* are compared with those produced by the downstream element of the class 2 alleles *S857*, *R134*, *S205*, and *X2092*, and the upstream element of the class 2 allele *R134*. Homozygotes (hom) as well as hemizygotes over the *W62* deletion allele are examined for each *an3* allele, and the corresponding phenotypes are indicated above the lanes as follows: m, an3^{mut} phenotype (spotted flower); (−), an3^{-} phenotype (white flower); and (+), An3^{+} phenotype (colored flower). The upper part of the gel shows the products that contain the *dTph1* insertion; the lower part shows the excision products. The excision products with wild-type size are marked WT, whereas the size of longer products is indicated with +6, +7, or +8 (bp).

excision product, because it was isolated from a somatically reverted branch (phenotypic selection for wild-type activity), whereas crosses showed that (germinal) excision of *dTph2* from *an3-GSm* virtually always results in stably inactivated *an3* alleles and rarely in *An3*$^+$ revertant alleles (data not shown).

The *an3* alleles *S205*, *R134*, *S857*, and *X2092* behaved quite differently and were therefore collectively designated as class 2 alleles. These four alleles all contain two *dTph1* elements at the *an3* locus (Figure 1). In general, self-pollinating homozygotes of any of these class 2 alleles yields ~50% of progeny with an an3^{mut} phenotype similar to the parental line and ~50% with an An3$^+$ revertant phenotype (data not shown). In progenies obtained by selfing *R134*/*R134* or *S205*/*S205* plants, we found at a low frequency (1 to 5%) plants with a very low spotting frequency (weakly an3^{mut}) that were often difficult to distinguish from a stable an3$^-$ phenotype. PCR analysis showed that such plants were always homozygous for the presence of the downstream *dTph1* element but could be either heterozygous or homozygous for the presence of the upstream element (Figure 1A; see hereafter for a detailed analysis). Because too few progeny were grown, we do not know if *X2092*/*X2092* or *S857*/*S857* also produce weak an3^{mut} progeny after self-pollination.

PCR experiments showed that in the *An3*$^+$ reversion alleles, the *dTph1* element upstream of the ATG remained present, whereas the *dTph1* copy downstream of the ATG was invariably lost. Sequencing of four *S205*-derived, two *R134*-derived, and one *S857*-derived (independent) germinal revertant alleles showed that the wild-type sequence had been perfectly restored at the empty donor sites in all seven cases. In another 24 somatic excision products recovered without phenotypic selection by PCR amplification from homozygous *S205*/*S205*, *R134*/*R134*, *S857*/*S857*, or *X2092*/*X2092* plants, we again found a perfect restoration of the wild-type sequence (Figure 2B). By contrast, sequencing of somatic and germinal excision products in which the upstream *dTph1* element in the *an3* alleles *S205*, *R134*, or *S857* had excised showed that these excision events had created footprints (Figure 2C).

These data indicate that elimination of the single *dTph1* element in a class 1 *an3* allele or the upstream *dTph1* element in a class 2 *an3* allele involves a ("classical") mechanism similar to that observed for transposons in snapdragon and maize. The downstream element of a class 2 *an3* allele, however, appears to be preferentially eliminated by a different ("novel") mechanism that yields products without a footprint.

Reversion of Class 2 Alleles Is Suppressed in Hemizygotes

Testcrosses between unstable *an3* mutants and lines harboring the *W62* deletion allele revealed yet another difference between unstable class 1 and class 2 *an3* alleles.

Crosses between homozygotes for an unstable class 1 *an3* allele and the *W62* allele yielded predominantly progeny with spotted (an3^{mut}) flowers (Table 1). The spotting frequency of such flowers always corresponded with that of the parental class 1 allele in the homozygous condition (Figures 3A and 3C). PCR analysis showed these an3^{mut} progeny plants contained the parental class 1 *an3* allele, including the *dTph1* element. *an3-W62* is a complete deletion, which implies that reversion of a class 1 allele is independent of *an3* sequences

Table 1. Genotypes and Phenotypes Produced by Crossing Unstable and Stable Recessive *an3* Mutants

	Number Of Progeny With Phenotype After Crossing With *An3*$^-$ Parent[a,b]														
an3^{mut}	*W62*			*S206*			*W1006*			*W2018FT*			*W29FT*		
Parent[a]	An3$^+$	an3^m	an3$^-$	An3$^+$	an3^m	an3$^-$	An3$^+$	an3^m	an3$^-$	An3$^+$	an3^m	an3$^-$	An3$^+$	an3^m	an3$^-$
W2018	0	**62**	6	0	**11**	21	0	**17**	0	0	**2**	2	0	**47**	6
W2298	0	**10**	7	–	–	–	–	–	–	–	–	–	0	**13**	0
W2303	0	**9**	8	10	**8**	0	–	–	–	–	–	–	10	**3**	3
W29	29	**63**	0	–	–	–	–	–	–	–	–	–	0	**20**	0
W2140	1	**17**	0	6	**10**	0	–	–	–	–	–	–	1	**14**	0
W2258	–	–	–	0	**18**	0	–	–	–	–	–	–	4	**4**	0
GSm	0	**19**	0	0	**5**	6	–	–	–	–	–	–	0	**4**	0
S205	155	0	**166**	46	0	**46**	6	0	**5**	7	0	**5**	68	0	**76**
S857	23	0	**13**	10	0	**13**	–	–	–	5	0	**3**	17	1[c]	**15**
R134	49	0	**38**	14	0	**14**	11	0	**7**	6	0	**11**	32	0	**34**
X2092	30	**21**	0	3	**6**	0	–	–	–	–	–	–	20	**25**	0

[a] All parental plants used were homozygous for the specific allele.

[b] For each phenotypic class, the number of progeny is given. Boldface numbers denote progeny harboring the unstable parental allele. The other numbers indicate progeny with derived excision alleles. A minus sign indicates that no data are available.

[c] Plant lacking the upstream *dTph1* element from S857: for details, see Table 2, family V2307, and accompanying text.

on the homologous chromosome. Other plants in the same progenies had evenly colored (An3$^+$) or nearly white flowers without spots (an3$^-$) (Figure 3B). PCR analysis showed that such plants always lacked the *dTph1* insertion in the class 1 allele, apparently due to an excision event in germinal cells of the parent. Depending on the sequence of the footprint and its position in the *an3* gene, such excision alleles have either a wild-type (An3$^+$) or a stable mutant (an3$^-$) phenotype.

Surprisingly, crosses between homozygotes for the three class 2 alleles, *S857*, *R134*, or *S205*, and *W62* yielded only An3$^+$ and an3$^-$ progeny (Figure 3F); the expected an3^{mut} phenotype was missing (Table 1). PCR analyses showed that the An3$^+$ plants lacked the downstream *dTph1* element of the class 2 allele, presumably as a result of germinal excision, whereas the an3$^-$ plants contained the parental class 2 allele, including both *dTph1* copies. We did not find an3$^-$ progeny containing an excision derivative of the class 2 allele with a footprint (Table 1), consistent with the finding that these excisions preferentially result in restoration of the

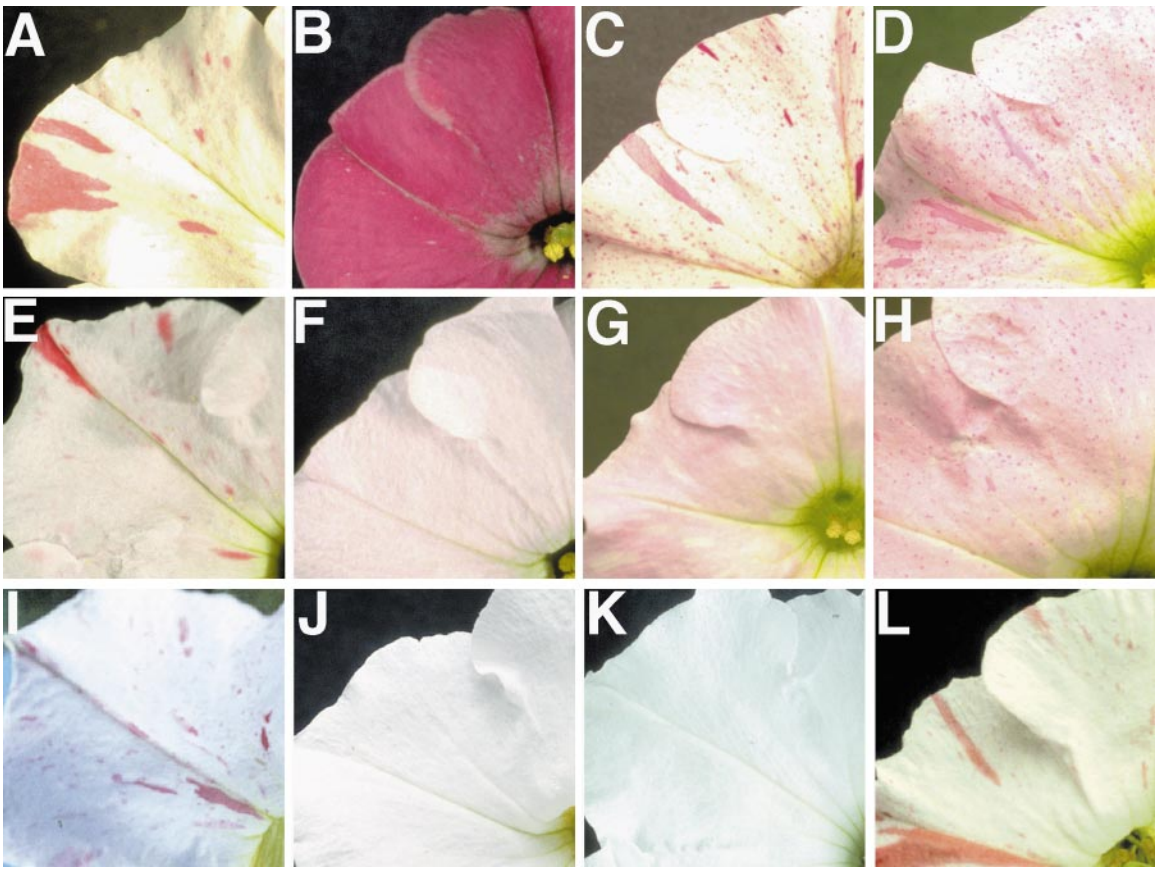

Figure 3. Phenotypes of Flowers with Different Combinations of *an3* Alleles.

(A) Flower of an *W2140*/*W2140* plant showing an an3^{mut} phenotype.
(B) Flower of an An3$^+$ plant harboring *an3-W62* and an An3$^+$ revertant allele derived from *an3-W2140*.
(C) Flower of a *W2140W62* plant showing an an3^{mut} phenotype.
(D) Flower of a *W2140*/*W29FT* showing an an3^{mut} phenotype.
(E) Flower of a homozygote for the *S857* allele (class 2) showing an an3^{mut} phenotype.
(F) Flower of an *S857*/*W62* heterozygote with an an3$^-$ phenotype due to suppression of *S857* instability.
(G) Flower of an *S857*/*W29FT* heterozygous plant from family V2307 (see Table 2) with an an3$^-$ phenotype.
(H) Flower of a *V2307* sibling plant with an an3^{mut} phenotype that is heterozygous for *W29FT* and a derivative allele of *S857* that lacks the upstream *dTph1* copy.
(I) Flower of an *S205*/*S205* plant showing an an3^{mut} phenotype.
(J) Flower of an *S205**/*V512* plant showing an an3$^-$ phenotype.
(K) Flower of an *S205**/*S205** plant showing an an3$^-$ phenotype.
(L) Flower of an *S205**/*S205* plant showing an an3^{mut} phenotype.

wild-type sequence (Figure 2B). The absence of revertant spots in hemizygotes for *an3*-*W62* and a class 2 *an3* allele indicates that in this F_1 background, reversions of the class 2 allele are somehow suppressed (cf. the flowers in Figures 3E and 3F).

The suppressed somatic reversion frequencies might be explained by (1) a decreased frequency of *dTph1* excision or (2) an alteration in the spectrum of excision products (to products that do not restore gene activity). To discriminate between these possibilities, we separated the complete array of PCR-amplified somatic excision products from class 1 and class 2 homozygotes and hemizygotes on high (1-bp) resolution gels. Using controls, we performed similar PCRs with plants harboring (stable) wild-type (Figure 2D, lanes 1, 5, 9, 13, 17, and 21) or germinal excision alleles (lanes 4, 8, 12, 16, and 20).

Figure 2D shows that the class 1 *an3* allele *W2018* generates predominantly excision products that are 7 bp longer than is the wild-type sequence (cf. lanes 1 and 2), which is consistent with the presence of footprints (cf. Figures 2A and 2D). When we used a cloned *W2018* DNA fragment as a template, these products were not detected, confirming that they result from in vivo transposon excisions and not from PCR artifacts (data not shown). In *W2018*/*W62* hemizygotes, no gross alterations in the spectrum of *W2018*-derived excision products were observed (Figure 2D, lane 3; note that *W62* is a complete deletion that does not generate PCR products). An $an3^{-}$ sibling from the same cross yielded only the *an3* fragment with a 7-bp footprint, whereas the *dTph1*-containing *an3* fragment was not detectable (Figure 2D, lane 4), indicating that *dTph1* had excised in germinal tissue of the *an3*-*W2018* parental plant. Similar results were obtained for other class 1 *an3* alleles (*W29*, *W2258*, *W2303*, *GSm*, and *W138A*; data not shown).

In homozygotes of the class 2 alleles *S857*, *R134*, and *S205*, excisions of the downstream element preferentially yielded products of a wild-type size (consistent with the absence of a footprint), although a small amount of slightly larger sized products was detectable (Figure 2D, lanes 6, 10, and 14). However, when the same alleles were hemizygous over the *W62* deletion, the wild-type-sized products were no longer detectable, whereas the larger excision products remained (Figure 2D, lane 7) or slightly increased in abundance (lane 11). The absence of wild-type excision products in these hemizygotes made it possible to clone and sequence some of the larger excision products. For *R134*/*W62* and *S857*/*W62* plants, this revealed that they contain a footprint similar to those in excision products of class 1 alleles (Figure 4). Because the downstream *dTph1* element in *S205*, *R134*, and *S857* is in the protein coding sequence, such footprints do not allow restoration of *an3* activity, explaining the absence of revertant spots in the flower.

At first sight, the fourth class 2 *an3* allele, *X2092*, seemed to behave differently from the three other class 2 alleles, because *X2092*/*W62* heterozygotes had spotted ($an3^{mut}$) flowers (Table 1) that were by phenotype (spotting frequency) indistinguishable from *X2092*/*X2092* homozygous flowers. Analysis of excision products showed that in *X2092*/*X2092* homozygotes, elimination of the downstream *dTph1* copy preferentially resulted in restoration of the wild-type *an3* sequence (Figure 2D, lane 18), although some slightly larger excision products were visible in longer gel exposures (data not shown). However, in *X2092*/*W62* hemizygotes, the wild-type-sized excision products were almost completely missing, and the 6- to 7-bp larger products increased in relative abundance (Figure 2D, lane 19). Thus, at the level of excision products, *X2092* behaves similarly to the other three class 2 alleles. The differences between the intron insertion (*X2092*) and the exon insertions (*S205*, *R134*, and *S857*) concern the phenotypic consequences of footprint formation. First, footprints in introns (as produced by hemizygous *X2092*) allow reversion of *an3* gene function and the formation of a colored spot, but footprints in exons (as produced by hemizygous *S205*, *S857*, or *R134*) in general do not. Second, the reduction of wild-type excision products in *X2092* hemizygotes is accompanied by a relatively strong increase in (reversion) products with a footprint, which can account for the relatively high reversion frequency seen in *X2092* hemizygous flowers.

We also examined excisions produced by the upstream element of the class 2 allele *R134*. Figure 2D shows that excisions of this *dTph1* copy yielded products that were longer than the wild-type sequence both in *R134*/*R134* homozygotes (lane 22) and in *R134*/*W62* hemizygotes (lane 23). Apparently, excisions of this *dTph1* element preferentially result in the formation of footprints independent of the homologous *an3* allele, similar to excision of the *dTph1* elements in class 1 alleles.

We conclude from these data that in homozygotes, the downstream *dTph1* element of a class 2 allele can be eliminated by either of two mechanisms. One mechanism, which is used infrequently, resembles the classical mechanism by which class 1 alleles revert, because it yields typical footprints and is not suppressed in a cross with the line W62.

Figure 4. Excision Products Generated by Class 2 *an3* Alleles in a Hemizygous Condition.

Sequence analysis of PCR-amplified somatic excision products produced by the downstream element of a class 2 *an3* allele in a hemizygous condition. Sequences of the wild-type allele, the class 2 allele harboring the *dTph1* insertion, and the excision products are as given in Figures 2A to 2C.

However, class 2 alleles revert preferentially by way of a second, novel mechanism that restores the wild-type sequence and becomes suppressed after a cross with W62.

Instability of Class 2 *an3* Alleles Is Homolog Dependent

The petunia lines W40 and W39 also contain the *W62* deletion allele, but they are in a different genetic background. Crosses between homozygotes of class 2 alleles and W40 or W39 also produced progeny in which reversions of the *S205*, *S857*, and *R134* allele were suppressed, making it unlikely that suppression was caused by an unknown gene in the background of these lines (data not shown). To test whether the observed suppression of class 2 reversions was due to the complete absence of *an3* sequences in line W62, we examined whether stable recessive *an3* alleles that retained different parts of the *an3* gene would cause suppression of class 2 reversions. Therefore, we crossed homozygotes for class 1 and class 2 unstable alleles with homozygotes for the alleles *S206* and *W1006*. Both of these *an3* alleles were isolated in the W138 background and contain relatively large chromosome rearrangements (inversion/translocation and a deletion, respectively), with breakpoints in the *an3* locus (Figure 1; van Houwelingen et al., 1998). These crosses produced progenies that were essentially similar to those produced by the crosses with W62 (Table 1). Each progeny plant was analyzed using PCR to determine which harbored the original class 1 or class 2 unstable *an3* allele and which harbored excision derivatives.

Table 1 shows that plants harboring a class 1 *an3* allele heterozygous with either *S206* or *W1006* have spotted flowers (an3^{mut}). By contrast, flowers that harbored one of the class 2 alleles *S857*, *R134*, or *S205* heterozygous with either *S206* or *W1006* were white (an3^{-}), indicating that reversions of the class 2 alleles were suppressed. Analysis of the PCR-amplified excision products produced by the downstream *dTph1* copy of *S857* and *R134* on high-resolution gels showed that excision products with a wild-type size were strongly reduced in heterozygotes with *S206* (data not shown), similar to the results described above for *S857* and *R134* hemizygotes. The fourth class 2 allele, *X2092*, specified an an3^{mut} phenotype when heterozygous with *W1006* or *S206*, similar to the *X2092*/*W62* hemizygotes described above.

Next, we crossed class 2 and class 1 alleles with plants harboring the *W2018FT* or *W29FT* alleles of *an3*. The two latter alleles were isolated as germinal excision derivatives of *W2018* and *W29*, respectively, and only contain small sequence alterations (footprints) in the otherwise intact *an3* gene (Figures 1 and 2A). The results of these crosses (Table 1) showed that *W29FT* and *W2018FT* also were capable of suppressing reversions of *S857*, *R134*, and *S205* in heterozygotes (see the example in Figure 3G) but not of *X2092* or any of the class 1 alleles (see the example in Figure 3D). These suppressed reversion frequencies were extended to germinal tissues because no An3^{+} revertants could be recovered in subsequent progeny of these plants (see below).

Because many of the *S205*/*S206* and *S857*/*S206* progeny were homozygous for the unstable *an1*-*W138* allele, we were able to examine whether reversions at another locus also were suppressed in the same plants. The *an1* locus controls transcription of a set of anthocyanin biosynthetic genes (Quattrocchio et al., 1993), and the unstable *an1*-*W138* allele contains a single 284-bp *dTph1* insertion that is eliminated by the classical mechanism, because footprints are generated upon its excision (C. Spelt and R. Koes, unpublished data). Because none of the *an3*$^{-}$ alleles blocks anthocyanin synthesis completely (even *W62*/*W62* flowers are very pale rather than completely white), we still were able to observe phenotypic reversions of the *an1*-*W138* allele (an1^{-} cells are completely white), even in an3^{-} plants. These observations were confirmed by PCR experiments, which also showed that the *dTph1* copy in *an1*-*W138* was still excising in somatic and germinal tissues of plants in which reversions of *S205*, *R134*, and *S857* were suppressed. Additional crosses (data not shown) demonstrated that the lines harboring *W62* and *S206* did not suppress the reversions of the *rt*-*Vu15* allele, which harbors a *dTph1* insertion at the *rhamnosylation at three* (*rt*) locus (Kroon et al., 1994).

In summary, these data show that any stable recessive *an3* allele can suppress reversions of a class 2 allele in trans-heterozygotes, making it unlikely that this suppression is due to the absence of *an3* sequences alone. Furthermore, these data show that the observed suppression is specific for class 2 *an3* alleles, because instability of *an1*, *rt*, and class 1 *an3* alleles is not suppressed in the same crosses.

Loss of the Upstream *dTph1* from a Class 2 Allele Results in a Novel Allele That Behaves as a Class 1 Allele

The four class 2 alleles all harbor two *dTph1* elements, suggesting that this structure may be responsible for their unusual behavior. If true, this predicts that loss of the upstream *dTph1* copy would change the genetic behavior of a class 2 allele into that of a class 1 allele. In five cases, our crosses yielded progeny with an exceptional phenotype that suggested that the original class 2 allele had indeed changed into a new allele with a class 1 behavior (Table 2). These plants were examined by PCR to determine the structure of the *an3* allele(s).

Family V2307, obtained from a cross between *S857*/*S857* and *W29FT*/*W29FT* parents, consisted of 17 An3^{+} plants (germinal revertants that had lost the downstream *dTph1* element of *S857*; data not shown), 15 an3^{-} plants (suppression of *S857* reversions; see Figure 3G), and one plant with an3^{mut} flowers (Figure 3H). Sequence analysis of PCR products amplified from the single an3^{mut} plant showed that the upstream *dTph1* element of *S857* had germinally excised, creating a 7-bp footprint (see Figure 2C, allele *V2307*),

Table 2. Conversion of Class 2 in Class 1 *an3* Alleles

	Parents	Progeny with Phenotype[a]		
Family	Unstable Allele × Stable Allele	An3$^+$	an3$^-$	an3^{mut}
V2307	*S857/S857* × *W29FT/W29FT*	17	**15**	1*
X2330	*R134/R134* × *W2018FT/W62*	13	**22**	1*
Z2046	*V512/S205* × *W62/W62*	0	**25**	21*
Z2045	*V512/S205* × *W29FT/W29FT*	0	**21**	17*
Z2345	*T3463/S205* × *W62/W62*	0	**6**	6*
V1519	*S205/S205* × *W62/W62*	6	**20**	1*[b]

[a] Boldface numbers denote plants that harbor the stabilized class 2 allele. The asterisks indicate plants in which the upstream *dTph1* copy of the corresponding class 2 *an3* allele is absent.
[b] Instability was noticed in selfed progeny of this plant.

whereas in the transposon sequences and the insertion site of the downstream element, no changes were observed (data not shown).

A similar phenomenon was seen in family X2330, originating from a cross between *R134*/*R134* and *W2018FT*/*W62* plants. This family consisted of 13 wild-type revertants (An3$^+$; resulting from excision of the downstream element of *an3-R134*), 22 plants with white flowers (an3$^-$, due to suppression of *R134* instability by the *W2018FT* or *W62* allele), and one plant with spotted flowers (an3^{mut}). Sequence analysis of the PCR-amplified *an3* allele in this plant showed that the upstream *dTph1* element of *R134* had excised, creating a 7-bp footprint (see Figure 2C, *X2330*). No alterations were found in the transposon sequences or the insertion site of the downstream element (data not shown).

Family V1519 was generated by crossing *S205*/*S205* and *W62*/*W62* parents at a time when we were still unaware of the upstream *dTph1* copy in the *S205* allele. PCR analysis showed that the six An3$^+$ plants contained a germinal excision derivative of *S205* that lacked the downstream *dTph1* copy, whereas this element was still present in the 21 progeny plants that were scored as an3$^-$. However, hindsight shows that one of these 21 must have displayed a low number of very small revertant spots (similar to the *V512*/*W62* and *T3463*/*W62* plants described below) that we did not notice at that time. After we had discovered the upstream *dTph1* copy, we reanalyzed the DNA samples from V1519 and found this element to be present in all progeny, except for one plant that had initially been (mis)scored as an3$^-$. We then germinated the seeds of this plant and obtained an3^{mut} progeny (data not shown), whereas self-pollinating *S205*/*W62* siblings from the V1519 family gave only an3$^-$ progeny (see below).

In two progenies obtained by self-pollination of *S205*/*S205* plants, heterozygous plants were identified (by PCR) that harbored *S205* and a derived excision allele lacking the upstream *dTph1* element (alleles *T3463* and *V512*; see Figures 1 and 5). Sequence analysis showed that *T3463* and *V512* contained a footprint at the former insertion site of this *dTph1* element (Figure 2C, *an3-T3462* and *an3-V512*), whereas no changes were observed in the sequence or insertion site of the downstream element (data not shown). When homozygous, the reversion frequency of the *T3463* and *V512* alleles was so low that it was barely detectable in the W138 (an1^{mut}) genetic background in which they were maintained. Therefore, *V512* and *T3463* are depicted as nearly stable recessive alleles in Figures 1 and 5. Electrophoretic analysis of the complete spectrum of excision products showed that excision of the downstream element from *S205* yielded, in the large majority of cases, a product of wild-type size and, at a much lower frequency, products with a footprint (Figure 6A, lanes 2 and 4). In *V512*/*V512* homozygotes, the wild-type-sized excision products were strongly diminished, but the excision products with a footprint were still detectable (Figure 6A, lane 5). The fraction of footprints (+3, +6, or +9 bp) that restore the reading frame and potentially allow reversion makes up a small fraction of the complete collection of footprints generated, thus explaining the low reversion frequency in *V512*/*V512* homozygotes. This indicates that *V512* now behaves as a typical class 1 allele.

To test whether *T3463* and *V512* displayed other features associated with class 1 alleles, we crossed *T3463*/*S205* and *V512*/*S205* heterozygotes to *W62*/*W62* homozygotes. In both cases, half of the progeny had weakly unstable (an3^{mut}) flowers (one to five small spots per flower, representing a low number of late reversions), whereas the flowers of the other half had no revertant spots at all and were scored an3$^-$ (Table 2, families Z2345 and Z2046, respectively). PCR analysis showed that all *S205*/*W62* progeny had an3$^-$ flowers, indicating suppression of *S205* reversions. The progeny with weakly unstable an3^{mut} flowers were genotypically *V512*/*W62* or *T3463*/*W62*. Similar results were obtained when the *V512*/*S205* plant was crossed to an *an3-W29FT* homozygote (Table 2, family Z2045). Apparently, the low reversion frequencies of *V512* and *T3463* (which are relatively easily detected in this *An1*$^+$ genetic background) are not suppressed by the *W62* or *W29FP* allele, whereas the high

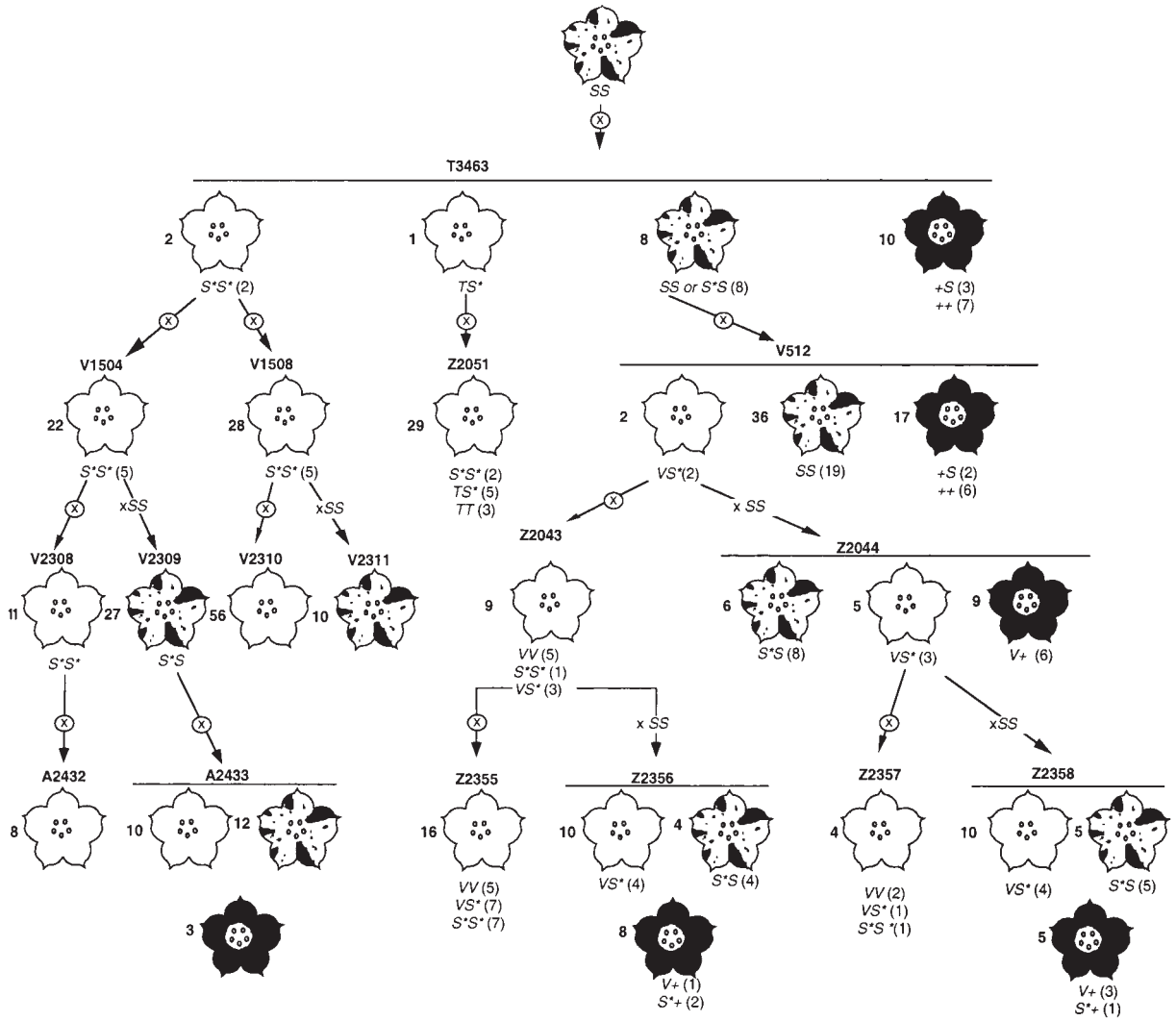

Figure 5. Genetic Analysis of the Suppression of *an3-S205* Instability.

Genetic analysis of the suppression of *an3-S205* by the derivative alleles *an3-T3463* and *an3-V512* is shown in the form of a pedigree. Each progeny (boldface numbers) resulted from a single pollination of parents with known genotypes, as indicated by the arrows. x denotes a self-fertilization; x*SS* denotes an outcross to unstable *S205*/*S205*. For each family, the flower phenotypes are shown as in Figures 1 and 3. For simplicity, the low numbers of revertant spots specified by *an3-T3463* and *an3-V512* are ignored and the corresponding phenotypes are indicated as white. For each phenotypic class, the genotype (determined by PCR) of several randomly selected individuals is shown in italics; for each genotype, the number of plants is given in parentheses. The different alleles are abbreviated as follows: *S*, *S205*; *S**, *S205** (suppressed reversions); *T*, *T3463*; *V*, *V512*; (+), revertant allele that lost the downstream *dTph1* copy of *S205*.

reversion frequency of *S205* is completely suppressed. However, when we compared the complete spectrum of PCR-amplified excision products in *S205*, *V512*, and *T3463* hemizygotes, we did not detect consistent differences that could account for the differing an3^{-} and weak an3^{mut} phenotypes (Figure 6A, lanes 6 to 9), most likely because the *V512*- or *T3463*-derived reversion products made up too small a fraction of the total amount of PCR products that were recovered in these assays.

Taken together, these data show that loss of the upstream *dTph1* element of a class 2 allele results in a new allele that genetically behaves as a class 1 allele, because (1) the frac-

tion of excision derivatives with wild-type sequence is strongly diminished and (2) it specifies spotted (an3^{mut}) flowers when heterozygous over a stable recessive *an3* allele.

Reactivation of Suppressed Class 2 Alleles

If the suppressed reversion of class 2 alleles in *trans*-heterozygotes is imposed by the stable recessive *an3* allele on the homologous chromosome, one would expect that the reversions are restored when the class 2 allele is made homozygous again. Therefore, we self-pollinated heterozygous plants harboring various combinations of the class 2 alleles *S857*, *R134*, and *S205* and the stable recessive alleles *W62*, *S206*, and *W1006* and analyzed the progeny (Table 3). Among a total of 777 progeny plants resulting from 24 different self-pollinations, no An3^{+} plants were found. This indicated that reversions of the class 2 alleles in the heterozygous parent were inhibited in germinal tissues of the parental plants, as they are in their somatic tissues.

Only 24 of these 777 progeny plants displayed some somatic An3^{+} reversions (i.e., spots). In all of these cases, *an3* instability appeared to be irregular, because we found on the same plant flowers with an3^{mut} and an3^{-} phenotypes. Furthermore, the number of revertant spots on an3^{mut} flowers was usually lower than the number on flowers of the parental class 2 homozygous lines. PCR analysis confirmed that all the plants bearing an3^{mut} flowers were indeed homozygous for the class 2 allele. However, the large majority of class 2 homozygotes (identified by PCR) remained phenotypically an3^{-} and did not show any An3^{+} reversions. This suggested that some unknown factor prevented the reactivation of instability in most (~85%) of the class 2 allele homozygotes.

Suppression of *an3-S205* Reversions Has Epigenetic Features

To gain further insight into the mechanism that prevents reversion of a class 2 allele, we focused on the interactions between the *S205* allele and the derived alleles *T3463* and *V512* (see Figures 1 and 2C for their structures). We selected these alleles for the following reasons. First, all three are in the same genetic background (W138). Second, suppression of *S205* reversions is very stable in progeny (Table 3). Third, the reversion frequency of *T3463* and *V512* is very low, enabling us to detect the relatively high reversion frequency of a *S205* allele in heterozygotes against a very low background of *V512*- or *T3463*-derived reversions. In fact, the *V512* and *T3463* reversion frequencies are completely negligible compared with those of *S205* (see Figures 3I to 3L); therefore, the *V512* and *T3463* flower phenotypes are, for simplicity, indicated as "white" (an3^{-}) in Figures 1 and 5.

The *V512* allele was identified in family V512 in a heterozygous (*V512*/*S205*) plant. This heterozygote had white flowers (an3^{-}), indicating that *V512* suppressed reversions of the *S205* allele on the homologous chromosome (cf. Figures 3I and 3J). Hereafter, we mark such a suppressed allele with an asterisk (*S205**) to differentiate it from a frequently reverting *S205* allele, even though we have not been able to detect structural differences between *S205* and *S205** (epi)alleles by using PCR or sequencing. The *V512*/*V512* and *V512*/*S205**

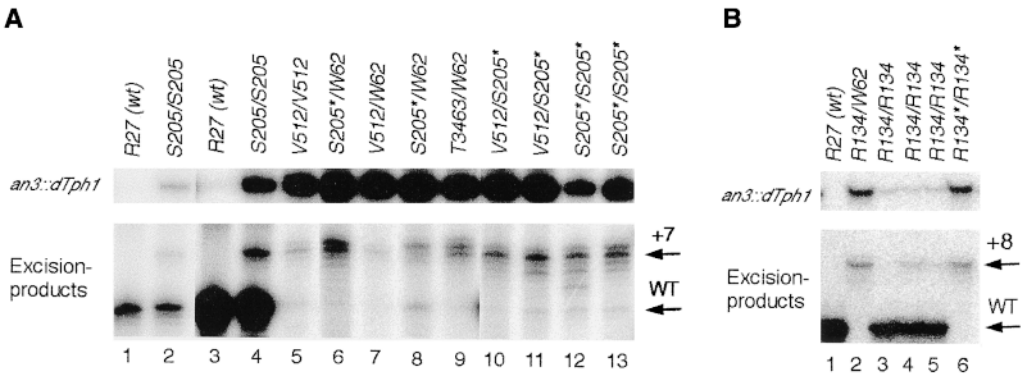

Figure 6. Spectrum of Excision Allele Products Generated by *an3-S205* and Derived (Epi)Alleles.

(A) PCR-amplified excision products produced by the downstream *dTph1* element of *S205*, the derived alleles *V512* and *T3463*, and the epiallele *S205** were separated on a 6% polyacrylamide gel. Homozygotes as well as heterozygotes over *an3-W62* were examined for each *an3* allele. Lanes 1 and 2 represent a short exposure of lanes 3 and 4.

(B) Excision products produced by the downstream *dTph1* of *R134* were analyzed as in **(A)**. The top part of the gel shows the products that contain the *dTph1* insertion; at bottom are the excision products. Major excision products with wild-type size or footprints are marked by WT and +7 or +8 (bp), respectively.

Table 3. Reactivation of Repressed *an3* Unstable Alleles

Parent Used for Self-Fertilization	No. of Distinct Parents Tested	Progeny with Phenotype[a]		
		An3$^+$	an3$^-$	an3^{mut}
an3-R134/an3-W1006	2	0	130	17
an3-R134/an3-W62	6	0	290	0
an3-S857/an3-W62	4	0	39	4
an3-S857/an3-S206	4	0	69	3
an3-S205/an3-W62	6	0	120	0
an3-S205/an3-S206	2	0	105	0
Total	24	0	753	24

[a] Plants in which only some flowers showed *an3* instability were scored an3^{mut}.

progeny obtained by self-pollinating this plant (family Z2043) had an3$^-$ flowers, as expected. Also, the *S205**/*S205** homozygote was an3$^-$ (Figure 3K), indicating that reversions were not reactivated after the *S205** allele was made homozygous again. When the same *V512*/*S205** parent was outcrossed to an *S205*/*S205* sibling with an an3^{mut} phenotype, the progeny segregated for An3$^+$, an3^{mut}, and an3$^-$ phenotypes (family Z2044). PCR analysis showed that the An3$^+$ plants were heterozygous for the downstream *dTph1* insertion, presumably due to a germinal reversion in the *S205*/*S205* parent. The an3$^-$ progeny were genotypically *V512*/*S205**, indicating that the *V512* allele again prevented reversions of the newly introduced *S205* allele (thus marked with an asterisk in Figure 5). The an3^{mut} progeny (see Figure 3L for an example) all appeared to be genotypically *S205**/*S205*.

Crosses with a *V512*/*S205** plant from family Z2043 gave the same result. After self-pollination, the *S205**/*S205** homozygotes were an3$^-$ (family Z2355), whereas outcrosses to an *S205*/*S205* plant yielded *S205**/*S205* progeny with an an3^{mut} phenotype (family Z2356). We also selected a *V512*/*S205** plant from family Z2044, in which suppression of *S205* reversion was established by an independent event. Again, self-pollinations yielded only an3$^-$ progeny (family Z2357), whereas outcrosses to an *S205*/*S205* plant with an an3^{mut} phenotype yielded an3^{mut} and An3$^+$ progeny (Z2358). The An3$^+$ progeny were all heterozygous for the downstream *dTph1* insertion, presumably due to a germinal reversion in the *S205*/*S205* parent.

The *T3463* allele has the same structure as *V512* (Figures 1 and 2C) but arose independently. In a heterozygote, *T3463* also suppressed reversions of *S205* (thus marked with an asterisk in Figure 5, family T3463), and this suppressed state was maintained when the *S205** allele was made homozygous again by selfing (family Z2051). Interestingly, two other plants in the T3463 family displayed an an3$^-$ phenotype. PCR analysis showed that they were both homozygous for an *an3* allele that was indistinguishable in structure from *S205*, except that somatic excision products were markedly decreased (data not shown). These suppressed *S205** alleles behaved in further crosses in a manner identical to the suppressed *S205** alleles described above. Thus, repeated self-fertilizations yielded only an3$^-$ progeny, even after three generations (families V2308, V2310, and progenies thereof), whereas outcrosses to homozygotes for an unstable *S205* allele produced an3^{mut} progeny (families V2309 and V2311). The simplest explanation for these results is that the *T3463* allele arose in germinal cells of the parental plant, leading to the suppression of reversions of the *S205* allele on the homologous chromosome and maintenance of this state in the gametes and progeny originating therefrom (family T3463).

It is possible that in the *S205**/*S205* heterozygous plants produced by the various outcrosses, both alleles contributed to the spotted an3^{mut} phenotype (implying that *S205** had converted back to *S205*) or that only *S205* contributed to the revertant spots, whereas *S205** remained in its stabilized state. Molecular analyses of the *S205*/*S205** heterozygotes themselves cannot distinguish between these possibilities, because excision products of either of the two alleles would have the same structure. Instead, we self-pollinated *S205*/*S205** plants from three different families to examine whether the stabilized *S205** could be recovered in the progeny. All resulting families (A2433 and data not shown) contained a high number of an3$^-$ plants, suggesting that the instability of the *S205** allele had not been reactivated in the *S205**/*S205* parent.

Similar to the crosses described above, 1 to 5% of the progeny resulting from self-fertilization of frequently reverting *R134*/*R134* plants exhibited a reversion frequency that was so low (i.e., weakly an3^{mut}) that it was difficult to distinguish from an an3$^-$ phenotype. PCR analysis of two such plants showed they were both homozygous for an *an3* allele that was indistinguishable from *R134*, except that the amounts of somatic excision products were markedly decreased (data not shown). This suggests that, in addition to *S205*, *R134* also could change into a "stabilized" (epi)allele, which we designated *R134**, analogous to the (epi)allele *S205**.

To analyze why the reversion frequencies became so strongly suppressed in *S205** and *R134** heterozygotes and homozygotes, we analyzed the spectrum of excision products produced by the downstream element. Figure 6A shows that in *S205**/*V512*, the fraction of wild-type-sized excision products was markedly reduced when compared with *S205*/*S205* homozygotes (cf. lanes 10 and 11 with lanes 2 and 4) and was of an essentially similar composition as that produced by *V512*/*V512* homozygotes (lane 5) or *V512*/*W62* hemizygotes (lane 7). Because in *S205**/*S205** homozygotes again a similar pattern of excision products was found (Figure 6A, lanes 12 and 13), we assume that *S205** and *V512* contribute similarly to the collection of excision products found in heterozygotes. These data indicate that the essential difference between *S205* and its derived epiallele *S205** is that the latter produces many fewer wild-

type-sized excision products, indicating that it has lost its capability to revert by the novel mechanism. Figure 6B shows that a frequently reverting *R134* allele in the homozygous condition produced mainly wild-type-sized excision products, whereas only a small fraction of the excision products contained an 8-bp footprint (lanes 3 to 5). However, in a homozygous *R134**/*R134** plant, the wild-type-sized excision products were markedly reduced, whereas the +8-bp footprint products remained detectable (Figure 6B, lane 6), similar to *R134*(*)/*W62* hemizygotes in which reversions were also suppressed (lane 2).

In summary, these data show that a frequently reverting class 2 allele such as *S205* undergoes heritable transition to a different "state" or epiallele (indicated as *S205**) in which reversions by the novel mechanism are suppressed if it is exposed to a derivative allele such as *V512* or *T3463* in a heterozygous cell. An *S205** allele, however, does not confer this state to an unstable *S205* allele in heterozygotes.

DISCUSSION

It is by now widely accepted that the activity of a gene is not determined by its sequence alone and that additional, epigenetic factors (e.g., changes in methylation or chromatin structure) can heritably modulate its expression (discussed in Martienssen and Richards, 1995; Riggs and Porter, 1996; Henikoff and Matzke, 1997; Lewin, 1998). The activity of transposon-encoded transposase genes can be subject to epigenetic regulation, as are immobile cellular genes. This regulation can be visualized by the presence or absence of revertant spots (reviewed in Fedoroff et al., 1995; Kunze et al., 1997). Here, we provide evidence that epigenetic mechanisms may also affect a DNA recombination mechanism involved in transposon excision and/or break repair. We show that a *dTph1* transposon can be eliminated from the host gene by either one (classical) or the other (novel) recombination mechanism and that the latter mechanism depends on a partially epigenetic interaction between at least three *dTph1* copies in two homologous chromosomes, as summarized in Figure 7.

Class 1 *an3* Alleles Revert by a Classical Mechanism

The genetic behavior of class 1 unstable *an3* alleles, harboring a single *dTph1* or *dTph2* insertion, is very similar to that of unstable alleles in other plants (Figure 7A). Excisions of *Ac* and *Ds* elements result, in the large majority of cases, in complete removal of transposon sequences and the formation of a footprint (Baran et al., 1992; Kunze et al., 1997). We refer to this mechanism of transposon excision and subsequent break repair as the classical mechanism. Most likely, the DSBs that excise the transposon occur by hairpin formation at the ends of the flanking DNA (Coen et al., 1986; Kennedy et al., 1998), but little is known about the mechanism by which the break in the chromosome is repaired. At a low frequency, *Ac*/*Ds* insertions produce excision alleles that lack a footprint, and it has been suggested that these may be formed by a distinct mechanism (Scott et al., 1996).

The simple class 1 *an3* alleles, harboring a single *dTph1* or *dTph2* insertion, behaved very similarly. In the majority of cases, transposon excision resulted in the formation of a footprint, whereas at a low frequency, excision alleles without a footprint could be found, especially when excision products were phenotypically selected (Figure 2A). Similar results were obtained with *dTph1* insertions at four other petunia loci (Souer et al., 1996, 1998; de Vetten et al., 1997; Alfenito et al., 1998). Furthermore, the footprints in maize, snapdragon, and petunia excision alleles all have a similar structure, consisting of remainders of the target site duplication that are often separated by inverted repetitions of the target site. Similar to other *Ac*-like transposons in plants, but unlike CACTA elements (Coen et al., 1986), *dTph1* and *dTph2* generate footprints that lack one nucleotide in the inverted repeat (Figure 2A; see also Souer et al., 1996, 1998; de Vetten et al., 1997; Alfenito et al., 1998).

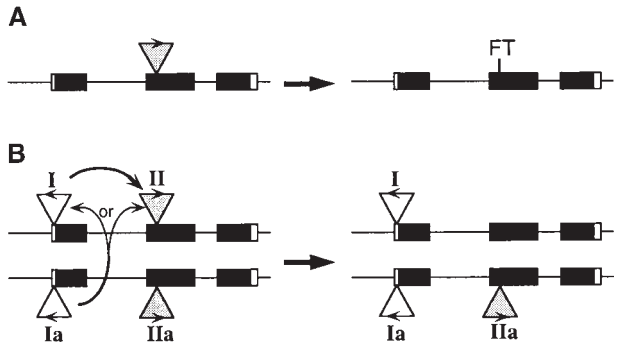

Figure 7. Diagram Summarizing the Genetic Behavior of Class 1 and Class 2 Unstable *an3* Alleles.

(A) Excision of the transposon from a class 1 *an3* allele. The excising *dTph1* element, indicated by a triangle, does not appear to interact with other elements and leaves a footprint (FT) behind at the empty donor site.

(B) Reversion of a class 2 *an3* allele. The two class 2 *an3* alleles are shown as they exist in a homozygous plant. The *dTph1* elements (numbered I, II, Ia, and IIa) are shown as triangles, and the arrowheads indicate their relative orientation. The boldface arrows indicate the (epi)genetic interactions between *dTph1* elements that result in the elimination of copy II by the "novel" mechanism and restoration of the wild-type sequence on the empty donor site. For simplicity, the symetrical interactions that lead to elimination of *dTph1* copy IIa have not been drawn. The exons of the *an3* gene are depicted by blocks, and the translated region is shown in gray.

Our results indicate that reversion of class 1 alleles is largely insensitive to the structure of the *an3* allele on the homologous chromosome. The absence of *an3* sequences on the homologous chromosome (as in hemizygotes with *an3-W62*) did not reduce the spotting frequency or cause alterations in the spectrum of excision products (Figure 2D). We also did not observe upregulation of the spotting frequency when intact *an3* sequences were present opposite the insertion sites (as in heterozygotes harboring the *S206* or *W29FT* allele). Thus, gene conversion mechanisms, like DSB repair, play at most a minor role in reversion of class 1 *an3* alleles.

Although a single *dTph1* insertion may in principle generate an array of different footprints, our data indicate that certain footprints are preferred over others. For instance, excision of *dTph1* from *W2018* preferentially results in a 7-bp footprint (Figures 2A and 2D) that causes a frameshift, consistent with the observation that most excisions result in a stable *an3*$^-$ allele (Table 1; data not shown). Yet, the revertant spots on *W2018* flowers show that different footprints, which restore *an3* function, also can occur but at a lower frequency. Analysis of a large number of *Ac* and *Ds* excisions from different positions at the maize *waxy* locus or Arabidopsis transgene(s) revealed a similar preference for certain footprints over others, which is determined at least in part by DNA sequences immediately flanking the transposon insertion (Scott et al., 1996; Rinehart et al., 1997). When a footprint is formed, its effect on the phenotype is also dependent on the position in the host gene; +7-bp footprints are tolerated in an intron but not in the coding sequence. Thus, two distinct phenomena, both dependent on the insertion site of the transposon, determine the actual reversion frequency, which can explain why different class 1 *an3* alleles display such enormously different reversion frequencies.

Class 2 *an3* Alleles Revert by a Novel Mechanism

Four unstable *an3* alleles, designated class 2, appear to revert by an unusual (novel) mechanism that differs from the classical reversion mechanism of class 1 alleles in several aspects (Figure 7B). First, the germinal reversion frequency of all class 2 alleles is very high (30 to 50%) compared with that of any of the class 1 alleles (Table 1). Second, in the large majority of excision products the wild-type sequence is restored and products with a footprint are very rare (Figure 2), explaining why the reversion frequencies of class 2 alleles vary so little with the insertion site. Third, the reversion frequency of class 2 alleles in germinal and somatic tissues depends on an interaction with the *an3* allele on the homologous chromosome (Table 1 and Figures 2, 3, and 5).

A homolog-dependent reversion frequency is the hallmark of the DSB repair mechanism by which transposon-excision gaps are repaired in the germ line of Drosophila and *C. elegans* (Engels et al., 1990; Plasterk, 1991). If reversion of a class 2 *an3* allele would involve DSB repair, the reversion frequency should depend on the *an3* sequences in the homologous *an3* allele, but this is apparently not the case. First, all stable recessive *an3* alleles, regardless of which *an3* sequences they contain, inhibit reversion of the class 2 *an3* allele in the homologous chromosome (Table 1). Second, the position of the mutation in the stable *an3*$^-$ allele, relative to the two *dTph1* insertions in the class 2 *an3* allele, does not seem to matter. For instance, in *W29FT*/*S205* heterozygotes, the *dTph1* copies are on either side relative to the lesion in *W29FT*, whereas in *W29FT*/*S857* or *W29FT*/*R134*, both *dTph1* copies are upstream of the footprint. Yet, both configurations result in suppressed reversion frequencies, whereas a DSB repair model would have predicted an increase. Third, in PCR assays designed to detect the conversion of marked sequences (e.g., the StuI restriction site created by the footprint in *W29FT*) from a stable recessive *an3* allele into the class 2 allele on the homologous chromosome, we could not detect gene conversion products (A. van Houwelingen and R. Koes, unpublished results). Although these data do not exclude the possibility that reversion of class 2 *an3* alleles requires *an3* sequences in the homologous chromosome, they do show that *an3* sequences alone are not sufficient. In fact, our data show that the class 2 allele senses a *dTph1* copy in the *an3* locus of the homologous chromosome (see below). None of these characteristics fits with a DSB repair model, implying that class 2 *an3* alleles revert by a different, novel mechanism.

Analysis of *Ds* excisions from six different positions in the maize waxy (*wx*) gene showed that one allele (*wx-C28*) produced predominantly excision alleles with a wild-type sequence (~66% of the excisions) rather than a footprint (~33% of the excisions), and this was taken as an indication that the two types of product were generated by two distinct mechanisms (Scott et al., 1996). It is possible that the *wx-C28* allele reverts by the same novel mechanism as the class 2 *an3* alleles described here. It will be interesting to determine if *wx-C28* contains, analogous to the class 2 *an3* alleles, a second *Ds* element at or near the *wx* locus and whether its reversion frequency is dependent on the *wx* allele in the homologous chromosome.

Reversion of a Class 2 *an3* Allele Requires an Interaction among at Least Three *dTph1* Elements

As outlined above, the reversion of class 2 *an3* alleles occurs by a novel mechanism that is distinct from the mechanisms of transposon excision and break repair discussed above. As a first step toward unraveling this mechanism, it is important to identify which components are involved and how they are involved. Figure 7B shows a generalized structure of the *an3* locus in a class 2 homozygote and summarizes the genetic interactions between different *dTph1* copies that appear essential for the elimination of one *dTph1* copy (copy II) by the novel mechanism.

The key feature that distinguishes class 2 *an3* alleles from class 1 alleles is the presence of a second *dTph1* insertion (copy I; Figure 7) that by itself does not affect the flower phenotype (although it does reduce the amount of *an3* transcripts; A. van Houwelingen and R. Koes, unpublished data). Several observations indicate that the elimination of *dTph1* copy II by the novel mechanism indeed depends on the presence of copy I in the same allele. First, excision of *dTph1* copy I from *S205* yields novel alleles (*V512* and *T3463*) with a barely detectable reversion frequency because they preferentially generate excision products with a footprint (Figure 6). Second, the spectrum of excision products does not show any major alterations when the *V512* allele is in a homozygous or hemizygous condition (Figure 6). Third, excision of *dTph1* copy I from three different class 2 alleles results in new alleles that specify an unstable ($an3^{mut}$) phenotype when heterozygous over a stable recessive *an3* allele (Figure 3H and Table 2). These data indicate that upon loss of *dTph1* element Ia (Figure 7), the class 2 allele changes its reversion behavior into that of a class 1 allele, which implies that *dTph1* copy I is required for the element downstream in the same allele (*dTph1* copy II) to be eliminated by the novel mechanism.

Strikingly, the interaction between *dTph1* copies I and II is not symmetrical. *dTph1* element I appears to be preferentially removed from a class II allele by the classical mechanism, because excisions result independently in footprints from the structure of the *an3* allele on the other chromosome (Figures 2C and 2D). Possibly, the directionality of this interaction is specified by the relative orientations of both *dTph1* copies, but because the relative orientation of *dTph1* copies is the same in all four class 2 *an3* alleles (Figure 1), we could not verify that experimentally.

Although the presence of *dTph1* copy I is necessary, it is clearly not sufficient to eliminate the downstream copy II by the novel mechanism, because sequences in the homologous *an3* allele also are required. The one common feature shared by all *an3* alleles that suppress reversions of a homologous class 2 allele in *trans* is the absence of *dTph1* element Ia, whereas the only *an3* allele that does not provoke the suppression, *S205**, does contain element Ia. The effect of *dTph1* copy Ia on the reversion frequency of the homologous allele is most clearly seen in plants in which the *S205*(*) allele is heterozygous over *V512* or *T3463*. In these heterozygotes, both the reversion frequency and the amount of wild-type-sized excision products are markedly decreased when compared with those in *S205*/*S205* homozygotes, indicating that neither *V512* (or *T3463*) nor *S205*(*) can revert by the novel mechanism. This implies that the absence of *dTph1* copy Ia (as in *V512* and *T3463*) does not affect only the elimination of the element downstream in the same allele (copy IIa) but also that of the downstream element (II) in the homologous *S205*(*) allele. Thus, elimination of *dTph1* element II somehow requires the presence of *dTph1* copy Ia on the homologous chromosome. However, we cannot conclude from our data whether this interaction is direct or indirect, for instance, via *dTph1* copy I (Figure 7).

To test whether *dTph1* copy II also senses *dTph1* copy IIa on the homologous chromosome, one needs to examine the instability of a class 2 allele in a heterozygote harboring an allele like *an3-W138A* or a reversion allele. The difficulty is that in such a plant, the reversion products produced by the class 2 alleles cannot be discerned (either by PCR or by phenotype) from the *an3* allele (*W138A* or *R27*) on the other chromosome.

Suppression of Class 2 Allele Reversions Fits the Genetic Definition of Paramutation

The phenomenon that one allele induces a directed and heritable alteration of the other allele in a heterozygote has been termed paramutation (Brink et al., 1968). In plants, several examples of paramutation are known, all of which concern the silencing of an endogenous gene (Hollick et al., 1997). Paramutation at the *r*, *b*, and *pl* loci of maize, all encoding regulators of the anthocyanin pathway, differs in several aspects, which suggests that distinct molecular mechanisms may fit the operational (genetic) definition of paramutation. For instance, paramutation at the (complex) *r* locus requires the presence of repeated gene sequences and results in an increased methylation of the paramutated allele (Kermicle et al., 1995). By contrast, paramutation of *b* and *pl* does not require gene repeats, and no alterations in the methylation pattern of paramutated *b* alleles could be detected (Hollick et al., 1995; Patterson et al., 1995).

Our data indicate that the interaction between *dTph1* copies II and Ia has an epigenetic character and that the inactivation of the novel excision repair mechanism by which a class 2 predominantly reverts fits the (genetic) definition of paramutation. When *dTph1* copy Ia is absent, the elimination of *dTph1* copy II from the homologous allele by the novel mechanism is suppressed and the class 2 allele undergoes a transition to a different "state" (essentially becoming a class 1 allele) that is heritable over at least three generations (Figures 2, 4, 5, and 6). How (methylation or otherwise?) and where (in *dTph1* and/or *an3* sequences?) the suppressed state of a class 2 allele is remembered remain to be determined.

The epigenetic suppression of the novel transposon excision–repair mechanism differs in several important aspects from the previously described examples of paramutation or epigenetic inactivation of transposons. First, the target process is not transcription of a transposase gene or an immobile gene but one or more steps in a DNA recombination process. Second, the epigenetic suppression specifically blocks elimination of the transposon by the novel mechanism, without blocking elimination by a second independent mechanism (the classical mechanism). Third, unlike paramutated *r*, *b*, or *pl* (epi)alleles, a paramutated (epi)allele such as *S205** does not change the behavior of a frequently reverting class 2 allele on the homologous chromosome.

METHODS

Genetic Analyses and Plant Material

The isolation and the molecular analysis of the unstable *anthocyanin3* (*an3*) alleles shown in Figure 1 have been described elsewhere (van Houwelingen et al., 1998). The *an3-W62* allele was maintained in three different *Petunia hybrida* lines (W62, W39, and W40). We used line W62 as a parent for crosses unless stated otherwise. Most *an3* alleles were isolated in line W138. This line also contains an unstable allele (*an1-W138*) at the *an1* locus. Some unstable *an3* alleles were maintained in an $an1^{mut}$ unstable background, whereas other alleles were maintained in an $An1^{+}$ revertant background. It was easy to distinguish instability of *an1* and *an3* because *an1* controls pigmentation in a cell-autonomous manner and produces revertant spots with a sharp border, whereas *an3* acts non-cell-autonomously and produces revertant spots with a fuzzy border (Koes et al., 1995; van Houwelingen et al., 1998). Because none of the mutant *an3* alleles blocks pigmentation completely (*an3* mutants have very pale flowers rather than pure white), *an1* instability was still detectable in $an3^{-}$ flowers.

All petunia plants were grown in a single greenhouse that was essentially free of pollinating insects. The plants used for this study were grown side by side with a wide array of other petunia lines, in use for other studies, that harbor mutations in various genes controlling the development and pigmentation of flowers and inflorescences. For crosses, we selected closed flower buds, which were still virgin because anthesis had not yet occurred; we then opened the corolla with a longitudinal cut, removed the anthers, and transferred pollen from another (open) flower of the same (self-pollination) or another (outcross) plant to the pistil. Subsequently, the fertilized flower was reclosed by wrapping a small rope around the corolla. Under these conditions, the opportunity for pollen contamination is virtually nonexistent.

For virtually every cross, we analyzed some of the progeny by polymerase chain reaction (PCR) to establish the *an3* genotype and, when necessary, the *an1* genotype. In case it was unclear whether two *dTph1* elements detected at the *an3* locus of transheterozygotes were in the same allele or in the two different alleles, the plant was crossed to an *an3-W62* homozygote and a number of (hemizygous) progeny analyzed by PCR.

DNA Methodology

Plant genomic DNA was extracted from leaves as described previously (Souer et al., 1995). PCR analysis of the *an3* locus was performed with primers complementary to appropriate regions of the *an3* locus, as described elsewhere (van Houwelingen et al., 1998).

Somatic excision products were isolated by PCR amplification of *an3* fragments from homozygotes with specific unstable *an3* alleles and cloned in pBluescript SK+ or SK− (Stratagene, La Jolla, CA). Recombinants that lacked transposon sequences were considered to originate from somatic excisions. Cloned excision products that had the same sequence were considered only to represent independent excision events when they had been amplified from different plants.

All sequencing was conducted by asymmetric PCR with fluorescent M13 primers, employing a DNA sequencer (model 370A; Applied Biosystems, Foster City, CA).

Analysis of Excision Products on Sequencing Gels

To analyze the full spectrum of excision products generated by a *dTph1* insertion, we performed a PCR reaction with primers flanking the transposon insertion. Amplification products were purified with Magic PCR Preps DNA Purification System (Promega) to remove excess primers. Subsequently, six (linear) amplification cycles were performed using 2 ng of purified fragment as a template and a single-nested primer that had been end labeled with phosphorus-32. The radiolabeled products were separated on 6% polyacrylamide (sequencing) gels, using sequence ladders of DNA fragments with a known sequence as a size marker. For each *an3* allele, this analysis was repeated with DNA preparations isolated from different plants to ensure that major excision products did not result from an occasional (early) excision event that had produced a large sector.

For the different *an3* alleles, the following primer combinations were used: an3-1, an3-12, and ^{32}P-labeled an3-5 for *an3-W2018*; an3-2, an3-5, and ^{32}P-labeled an3-14 for *an3-S857*; an3-1, an3-12, and ^{32}P-labeled an3-5 for *an3-R134*; an3-11, an3-12, and ^{32}P-labeled an3-6 for *an3-S205*; an3-13, an3-6, and ^{32}P-labeled an3-8 for *an3-X2092*; and an3-4, an3-14, and ^{32}P-labeled an3-3 for the upstream element in *an3-R134*.

The sequences of the primers are as follows: an3-5, 5′-CGGGATCCTGTAGATGGCTAGAGAC-3′; an3-6, 5′-CGGGATCCTTCTCCAAGCCCATAG-3′; an3-11, 5′-GGGCAAGAGACTACTCTAGATG-3′; an3-13, 5′-CTTCACATTTGTCTTCCGAG-3′; and an3-8, 5′-GGAATTCCTTTATTACGTGTTTGCGG-3′. The sequences of the other primers have been described elsewhere (van Houwelingen et al., 1998).

ACKNOWLEDGMENTS

We thank Toon Stuitje and Maike Stam for critical comments on the manuscript. We are grateful to Daisy Kloos for her assistance in the genetic experiments, to Pieter Hoogeveen and Martina Meesters for their care of the plants, and to Wim Bergenhenegouwen and Fred Schuurhof for photography. This research was supported by The Netherlands Technology Foundation (STW), with financial aid from The Netherlands Organization for the Advancement of Research (NWO).

Received December 7, 1998; accepted April 12, 1999.

REFERENCES

Agrawel, A., Eastman, Q.M., and Schatz, D.G. (1998). Transposition mediated by RAG1 and RAG2 and its implications for the evolution of the immune system. Nature **394,** 744–751.

Alfenito, M.R., Souer, E., Goodman, C.D., Buell, R., Mol, J., Koes, R., and Walbot, V. (1998). Functional complementation of anthocyanin sequestration in the vacuole by widely divergent glutathione *S*-transferases. Plant Cell **10,** 1135–1149.

Banks, J.A., Masson, P., and Fedoroff, N. (1988). Molecular mechanisms in the developmental regulation of the maize *Suppressor-mutator* transposable element. Genes Dev. **2,** 1364–1380.

Baran, G., Echt, C., Bureau, T., and Wessler, S. (1992). Molecular analysis of the maize *wx-B3* allele indicates that precise excision of the transposable element *Ac* is rare. Genetics **130,** 377–384.

Brink, R.A., Styles, E.D., and Axtell, J.D. (1968). Paramutation: A directed genetic change. Science **159,** 161–170.

Brutnell, T.P., and Dellaporta, S.L. (1994). Somatic inactivation and reactivation of *Ac* associated with changes in cytosine methylation and transposase expression. Genetics **138,** 213–225.

Brutnell, T.P., May, B.P., and Dellaporta, S.L. (1997). The *Ac-st2* element exhibits a positive dosage effect and epigenetic regulation. Genetics **147,** 823–834.

Chen, J., Greenblatt, I.M., and Dellaporta, S.L. (1992). Molecular analysis of *Ac* transposition and DNA replication. Genetics **130,** 665–676.

Coen, E.S., Carpenter, R., and Martin, C. (1986). Transposable elements generate novel spatial patterns of gene expression in *Antirrhinum majus*. Cell **47,** 285–296.

Craig, N.L. (1995). Unity in transposition reactions. Science **270,** 253–254.

de Vetten, N., Quattrocchio, F., Mol, J., and Koes, R. (1997). The *an11* locus controlling flower pigmentation in petunia encodes a novel WD-repeat protein conserved in yeast, plants and animals. Genes Dev. **11,** 1422–1434.

Engels, W.R. (1996). P-elements in Drosophila. In Transposable Elements, H. Saedler and A. Gierl, eds (Berling: Springer-Verlag), pp. 103–123.

Engels, W.R., Johnson-Schlitz, D.M., Eggleston, W.B., and Sved, J. (1990). High frequency P element loss in Drosophila is homolog dependent. Cell **62,** 515–526.

Fedoroff, N.V. (1989). The heritable activation of cryptic *Suppressor-mutator* elements by an active element. Genetics **121,** 591–608.

Fedoroff, N., Schläppi, M., and Raina, R. (1995). Epigenetic regulation of the maize *Spm* transposon. Bioessays **17,** 291–297.

Gerats, A.G.M., Huits, H., Vrijlandt, E., Maraña, C., Souer, E., and Beld, M. (1990). Molecular characterization of a nonautonomous transposable element (*dTph1*) of petunia. Plant Cell **2,** 1121–1128.

Gloor, G.B., Nassif, N.A., Johnson-Schlitz, D.M., Preston, C.R., and Engels, W.R. (1991). Targeted gene replacement in *Drosophila* via P element–induced gap repair. Science **253,** 1110–1117.

Henikoff, S., and Matzke, M.A. (1997). Exploring and explaining epigenetic effects. Trends Genet. **13,** 293–294.

Hiom, K., Melek, M., and Gellert, M. (1998). DNA transposition by the RAG1 and RAG2 proteins: A possible source of oncogenic translocations. Cell **94,** 463–470.

Hollick, J.B., Patterson, G.I., Coe, E.H., Cone, K.C., and Chandler, V.L. (1995). Allelic interactions heritably alter the activity of a metastable maize *pl* allele. Genetics **141,** 709–719.

Hollick, J.B., Dorweiler, J.E., and Chandler, V.L. (1997). Paramutation and related allelic interactions. Trends Genet. **13,** 302–308.

Hsia, A.P., and Schnable, P.S. (1996). DNA sequence analyses support the role of interrupted gap repair in the origin of internal deletions of the maize transposon, *MuDR*. Genetics **142,** 603–618.

Hudson, A., Carpenter, R., and Coen, E. (1987). De novo activation of the transposable element *Tam2* of *Antirrhinum majus*. Mol. Gen. Genet. **207,** 54–59.

Huits, H.S.M., Koes, R.E., Wijsman, H.J.W., and Gerats, A.G.M. (1994). Genetic characterization of *Act1* the activator of a non-autonomous transposable element from *Petunia hybrida*. Theor. Appl. Genet. **91,** 110–117.

Johnson-Schlitz, D.M., and Engels, W.R. (1993). P-element induced interallelic gene conversion of insertions and deletions in *Drosophila melanogaster*. Mol. Cell. Biol. **13,** 7006–7018.

Kennedy, A.K., Guhathakurta, A., Kleckner, N., and Haniford, D.B. (1998). Tn*10* transposition via a DNA hairpin complex. Cell **95,** 125–134.

Kermicle, J.L., Eggleston, W.B., and Alleman, M. (1995). Organization of paramutagenicity in *R-stippled* maize. Genetics **141,** 361–372.

Koes, R., et al. (1995). Targeted gene inactivation in petunia by PCR-based selection of transposon insertion mutants. Proc. Natl. Acad. Sci. USA **81,** 8149–8153.

Krebbers, E., Hehl, R., Piotrowiak, R., Lönnig, W.-E., Sommer, H., and Saedler, H. (1987). Molecular analysis of paramutant plants of *Antirrhinum majus* and the involvement of transposable elements. Mol. Gen. Genet. **209,** 499–507.

Kroon, J., Souer, E., de Graaff, A., Xue, Y., Mol, J., and Koes, R. (1994). Cloning and structural analysis of the anthocyanin pigmentation locus *Rt* of *Petunia hybrida*: Characterization of insertion sequences in two mutant alleles. Plant J. **5,** 69–80.

Kunze, R., Saedler, H., and Lönnig, W.-E. (1997). Plant transposable elements. Adv. Bot. Res. **27,** 331–469.

Lewin, B. (1998). The mystique of epigenetics. Cell **93,** 301–303.

Lisch, D., Chomet, P., and Freeling, M. (1995). Genetic characterization of the *Mutator* system in maize: Behavior and regulation of *Mu* transposons in a minimal line. Genetics **139,** 1777–1796.

Martienssen, R.A., and Richards, E.J. (1995). DNA methylation in eukaryotes. Curr. Opin. Genet. Dev. **5,** 234–242.

Mathern, J., and Hake, S. (1997). *Mu*-element-generated gene conversions in maize attenuate the dominant knotted phenotype. Genetics **147,** 305–314.

Oetinger, M.A., Schatz, D.G., Gorka, C., and Baltimore, D. (1990). RAG1 and RAG2 adjacent genes that synergistically activate V(D)J recombination. Science **248,** 1517–1523.

Patterson, G.I., Kubo, K.M., Shroyer, T., and Chandler, V.L. (1995). Sequences required for paramutation of the maize *b* gene map to a region containing the promoter and upstream sequences. Genetics **140,** 1389–1406.

Plasterk, R.H.A. (1991). The origin of footprints of the *Tc1* transposon of *Caenorhabditis elegans*. EMBO J. **10,** 1919–1925.

Quattrocchio, F., Wing, J.F., Leppen, H.T.C., Mol, J.N.M., and Koes, R.E. (1993). Regulatory genes controlling anthocyanin pigmentation are functionally conserved among plant species and have distinct sets of target genes. Plant Cell **5,** 1497–1512.

Riggs, A.D., and Porter, T.N. (1996). Overview of epigenetic mechanisms. In Epigenetic Mechanisms of Gene Regulation, V.E.A. Russo, R.A. Martienssen, and A.D. Riggs, eds (Cold Spring Harbor, NY: Cold Spring Harbor Laboratory Press), pp. 29–45.

Rinehart, T.A., Dean, C., and Weil, C.F. (1997). Comparative analysis of non-random DNA repair following *Ac* transposition in maize and *Arabidopsis*. Plant J. **12,** 1419–1427.

Rommens, C.M.T., van Haaren, M.J.J., Nijkamp, H.J.J., and Hille, J. (1993). Differential repair of excision gaps generated by transposable elements of the '*Ac* family.' Bioessays **15,** 507–512.

Roth, D.B., and Craig, N.L. (1998). VDJ recombination: A transposase goes to work. Cell **94,** 411–414.

Schläppi, M., Raina, R., and Fedoroff, N. (1994). Epigenetic regulation of the maize *Spm* transposable element: Novel activation of a methylated promoter by TnpA. Cell **77,** 427–437.

Schwartz, D. (1989). Gene-controlled cytosine demethylation in the promoter region of the *Ac* transposable element. Proc. Natl. Acad. Sci. USA **86,** 2789–2793.

Scott, L., Lafoe, D., and Weil, C.F. (1996). Adjacent sequences influence DNA repair accompanying transposon excision in maize. Genetics **142,** 237–246.

Souer, E., Quattrocchio, F., de Vetten, N., Mol, J.N.M., and Koes, R.E. (1995). A general method to isolate genes tagged by a high copy number transposable element. Plant J. **7,** 677–685.

Souer, E., van Houwelingen, A., Kloos, D., Mol, J.N.M., and Koes, R. (1996). The *no apical meristem* gene of petunia is required for pattern formation in embryos and flowers and is expressed at meristem and primordia boundaries. Cell **85,** 159–170.

Souer, E., van der Krol, A.R., Kloos, D., Spelt, C., Bliek, M., Mol, J., and Koes, R. (1998). Genetic control of branching pattern and floral identity during *Petunia* inflorescence development. Development **125,** 733–742.

van Gent, D.C., McBlane, J.F., Ramsden, D.A., Sadofsky, M.J., Hesse, J.E., and Gellert, M. (1995). Initiation of V(D)J recombination in a cell-free system. Cell **81,** 925–934.

van Gent, D.C., Mizuuchi, K., and Gellert, M. (1996). Similarities between initiation of V(D)J recombination and retroviral integration. Science **271,** 1592–1594.

van Houwelingen, A., Souer, E., Spelt, C., Kloos, D., Mol, J., and Koes, R. (1998). Analysis of flower pigmentation mutants generated by random transposon mutagenesis in *Petunia hybrida*. Plant J. **13,** 39–50.